© 2018. Published by The Company of Biologists Ltd | Journal of Cell Science (2018) 131, jcs216101. doi:10.1242/jcs.216101

RESEARCH ARTICLE

Wnt7b signalling through Frizzled-7 receptor promotes dendrite development by coactivating CaMKII and JNK

María E. Ferrari[1,2], María E. Bernis[2,3,*], Faye McLeod[4], Marina Podpolny[4], Romina P. Coullery[1,2], Inelia M. Casadei[1,2,‡], Patricia C. Salinas[4] and Silvana B. Rosso[1,2,§]

ABSTRACT

The formation of complex dendritic arbors is crucial for the assembly of functional networks as abnormal dendrite formation underlies several neurodevelopmental and psychiatric disorders. Many extracellular factors have been postulated as regulators of dendritic growth. Wnt proteins play a critical role in neuronal development and circuit formation. We previously demonstrated that Wnt7b acts through the scaffold protein dishevelled 1 (Dvl1) to modulate dendrite arborisation by activating a non-canonical Wnt signalling pathway. Here, we identify the seven-transmembrane frizzled-7 (Fz7, also known as FZD7) as the receptor for Wnt7b-mediated dendrite growth and complexity. Importantly, Fz7 is developmentally regulated in the intact hippocampus, and is localised along neurites and at dendritic growth cones, suggesting a role in dendrite formation and maturation. Fz7 loss-of-function studies demonstrated that Wnt7b requires Fz7 to promote dendritic arborisation. Moreover, *in vivo* Fz7 loss of function results in dendritic defects in the intact mouse hippocampus. Furthermore, our findings reveal that Wnt7b and Fz7 induce the phosphorylation of Ca^{2+}/calmodulin-dependent protein kinase II (CaMKII) and JNK proteins, which are required for dendritic development. Here, we demonstrate that Wnt7b–Fz7 signals through two non-canonical Wnt pathways to modulate dendritic growth and complexity.

KEY WORDS: Wnt signalling, Fz receptor, Dendrite development, Neuron, CaMKII, JNK

INTRODUCTION

Neurons are highly polarised cells exhibiting a single long axon, which transmits information, and complex dendrites that specialise in receiving and integrating signals (Witte and Bradke, 2008; Conde and Cáceres, 2009). Dendrite formation and maturation are critical processes required for proper neuronal connectivity and function. Indeed, abnormal dendritic development and arborisation correlate with neuropathologies, such as mental retardation and Down or Fragile X syndromes (Kaufmann and Moser, 2000; Fiala et al., 2002; Zoghbi, 2003). During development, secreted factors modulate dendritic growth and branching by triggering signalling pathways that affect neuronal cytoskeleton and gene expression (Valnegri et al., 2015). For example, secreted factors such as bone morphogenetic protein 7 (BMP7) and semaphorin 3A (Sema3A) affect dendrite outgrowth and orientation by regulating actin dynamics (Withers et al., 2000; Lee-Hoeflich et al., 2004). In addition, Sema3A differentially guides axons and dendrites, and modulates dendrite architecture (Shelly et al., 2011). Sema3A-null mice exhibit a reduction in dendritic length and branching in cortical neurons (Fenstermaker et al., 2004). Furthermore, brain-derived neurotrophic factor (BDNF) induces a significant increase in the length and complexity of dendrites in hippocampal neurons (Ji et al., 2005; Kellner et al., 2014; Baj et al., 2016). These findings demonstrate that different signalling factors modulate dendritic development and the final architecture of the dendritic arbor.

Wnt secreted factors are cysteine-rich glycoproteins that interact with different families of receptors, such as the seven transmembrane Fz receptors, the co-receptors from the family of low-density lipoprotein receptor-related proteins (LRP5/6), and the two atypical tyrosine-kinase receptors Ror and Ryk (Keeble and Cooper, 2006; Angers and Moon, 2009; Ho et al., 2012; Clark et al., 2014). These secreted proteins are crucial regulators of dendrite formation, maintenance and function (Yu and Malenka, 2003; Rosso et al., 2005; Ciani et al., 2011; Rosso and Inestrosa, 2013). In this context, we previously demonstrated that Wnt7b, through dishevelled 1 (Dvl1), modulates dendrite development and complexity by activating Rac and JNK (Rosso et al., 2005). However, the specific receptor through which Wnt7b controlled dendrite formation was unknown.

In this study, we identify the Wnt7b receptor involved in dendritogenesis and analyse the contribution of Ca^{2+}/calmodulin-dependent protein kinase II (CaMKII)-mediated non-canonical signalling. We report that Wnt7b binds to the extracellular domain of Fz7 (also known as FZD7), a receptor that is dynamically expressed during development. Gain-of-function studies demonstrate that Fz7, like Wnt7b, increases dendritic length and branching. Importantly, loss of Fz7 in mice or blockage of Fz7 expression in cultured neurons leads to abnormal dendrite architecture. Moreover, we demonstrated that Wnt7b also signals through Fz7 and Dvl1 to regulate the formation and maturation of dendrites by activating CaMKII. Taking into account our previous work on Wnt7b (Rosso et al., 2005), we further examined whether JNK functions downstream of Fz7. Indeed, we demonstrate that Wnt7b-Fz7 signals through JNK pathway to modulate dendrite morphogenesis. Conversely, inhibition of CaMKII or JNK abolishes the function of Wnt7b-Fz7 on dendrites. Thus, our studies identify, for the first time, the Wnt7b receptor necessary for dendrite development. Importantly, our findings describe the signalling pathway triggered by Wnt7b and its receptor Fz7 that modulate dendritic growth and complexity.

[1]Laboratorio de Toxicología Experimental, Facultad de Ciencias Bioquímicas y Farmacéuticas, Universidad Nacional de Rosario, Argentina. [2]Consejo Nacional de Investigaciones Científicas y Técnicas (CONICET), 2000 - Rosario, Argentina. [3]Departamento de Química Biológica-CIQUIBIC, Facultad de Ciencias Químicas, Universidad Nacional de Córdoba-CONICET, 5000 - Córdoba, Argentina. [4]Department of Cell and Developmental Biology, University College London, London WC1E 6BT, UK. *Present Address: German Center for Neurodegenerative Diseases (DZNE), 53127 Bonn, Germany. ‡Present Address: Instituto de Investigaciones en Medicina Traslacional, CONICET, Universidad Austral, Argentina.

§Author for correspondence (srosso@fbioyf.unr.edu.ar)

M.E.F., 0000-0001-7427-6702; R.P.C., 0000-0002-2366-7903; S.B.R., 0000-0003-1137-2689

Received 30 January 2018; Accepted 29 May 2018

Journal of Cell Science (2018) 131, jcs216101. doi:10.1242/jcs.216101

RESULTS

Fz7 is expressed during dendrite development in the hippocampus

To understand the signalling mechanisms involved in Wnt7b-mediated dendritogenesis (Rosso et al., 2005), we first examined the temporal expression of Fz7 in the developing hippocampus and in cultured pyramidal neurons at different developmental stages. We observed very low expression of Fz7 at embryonic day (E)19 and postnatal day (P)0; however, the levels increased at later stages, reaching the highest expression in the adult hippocampus (Fig. 1A, left panel). To begin studying the involvement of Fz7 in dendrite formation, we also examined the temporal expression of Fz7 in hippocampal neurons at 2, 6 and 10 days *in vitro* (DIV). We observed an increase of Fz7 levels during development, concomitant with an increase of PSD-95 (also known as DLG4; a postsynaptic marker highly expressed in mature neurons) (Fig. 1A, right panel). Next, we examined temporal and spatial distribution of Fz7 in neurons through immunofluorescence staining. At an early developmental stage (1 DIV), endogenous Fz7 was distributed mostly in the cell body and along immature processes, and was also concentrated at the growth cones of short neurites (Fig. 1B, left panel). This finding suggests that Fz7 likely modulates neurite elongation and growth. Furthermore, analysis of polarised neurons showed that Fz7 was present in the cell body and along neurites (Fig. 1B, middle panel). Importantly, double immunolabelling with the axon marker Tau1 revealed that Fz7 was present in the axon and along Tau1-negative neurites, which will later become dendrites. In more mature neurons (4 DIV), the Fz7 receptor was present at the cell body and along dendrites, colocalising with the dendritic marker Map2 (Fig. 1B, right panel). Thus, the endogenous Fz7 localisation in dendrites suggests that it a possible role in dendritic development.

Wnt7b binds to Fz7

Previously, we demonstrated that Wnt7b modulates the dendrite morphology of hippocampal pyramidal neurons through a non-canonical Wnt signalling pathway (Rosso et al., 2005). However, the receptor mediating this Wnt7b effect was unknown. To study whether Wnt7b interacts with Fz7, we first performed immunoprecipitation (IP) experiments using HEK293 cells

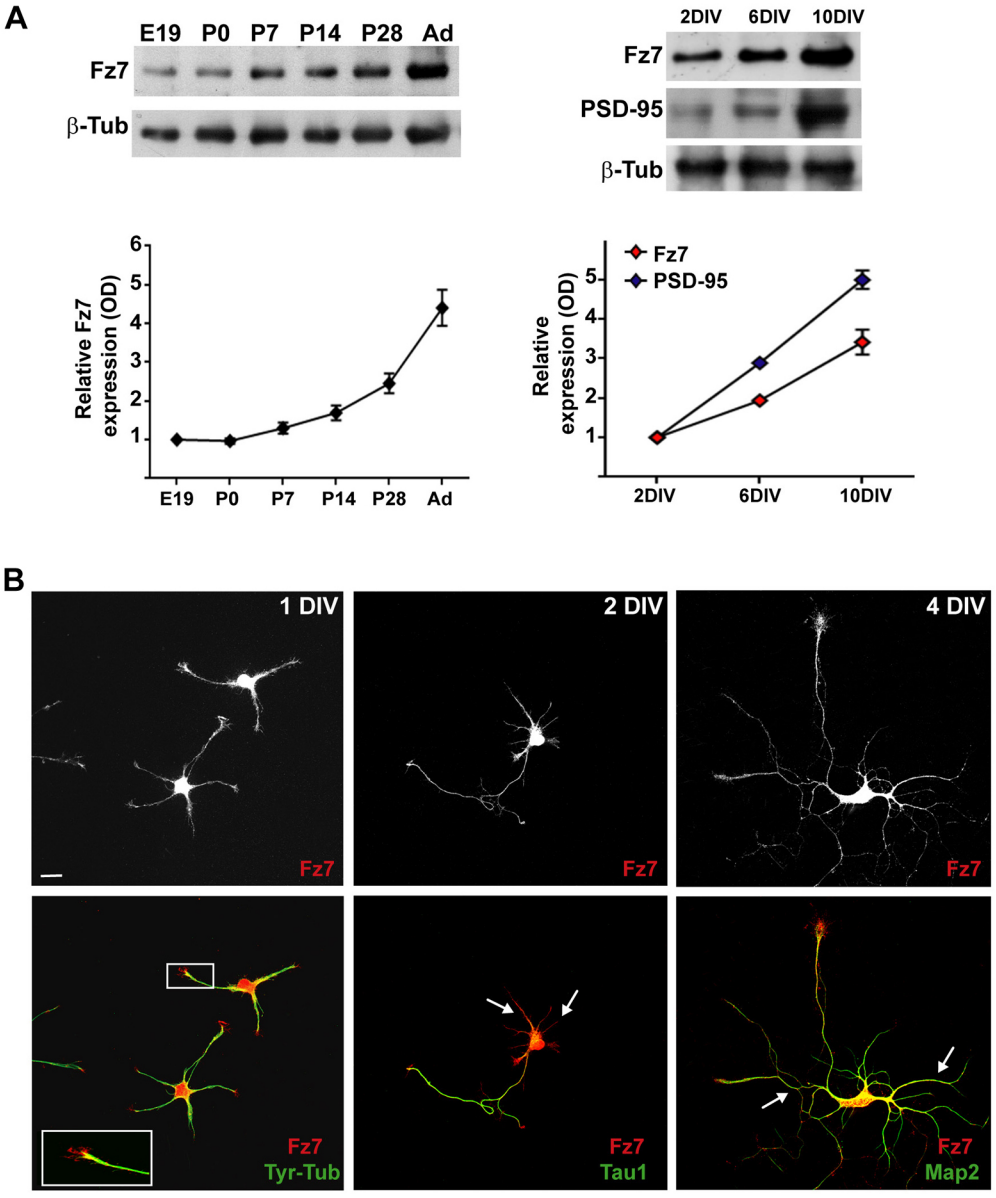

Fig. 1. Fz7 is expressed in both the hippocampus and hippocampal pyramidal neurons during development. (A) Western blotting of extracts of cells from the hippocampus of E19, P0, P7, P14, P28 and adult rats (left panel) and from dissociated hippocampal neurons at 2, 6 and 10 DIV (right panel) showing the expression level of Fz7 during development. PSD-95 expression is also shown. Class III β-tubulin was used as loading control. The quantification shows the relative optical densities (OD) of Fz7 to β-tubulin. Data was obtained from five independent experiments. Error bars represent mean ±s.e.m. (B) Immunofluorescence images showing the localisation of Fz7 in dissociated hippocampal neurons at 1, 2 and 4 DIV. Cells were labelled for Fz7 (red) and tyrosinated α-tubulin (Tyr-Tub), Map2 (green) or Tau1 (green). Note Fz7 localises along neurites (arrows) and at the growth cones of minor processes (inset, left panel). Scale bar: 10 µm.

Journal of Cell Science (2018) 131, jcs216101. doi:10.1242/jcs.216101

co-expressing Wnt7b–HA and Fz7–Myc constructs. The results revealed that Fz7 formed a complex with Wnt7b, as Fz7 was able to co-immunoprecipitate with Wnt7b (Fig. 2A). Additionally, we examined whether Wnt7b could interact with Ror2, a tyrosine kinase Wnt receptor. We did not observe co-immunoprecipitation of Ror2 and Wnt7b (Fig. 2A, lower panel).

Previous studies have shown that Wnt ligands bind to the N-terminal cysteine-rich domain (CRD) of Fz receptors and that this

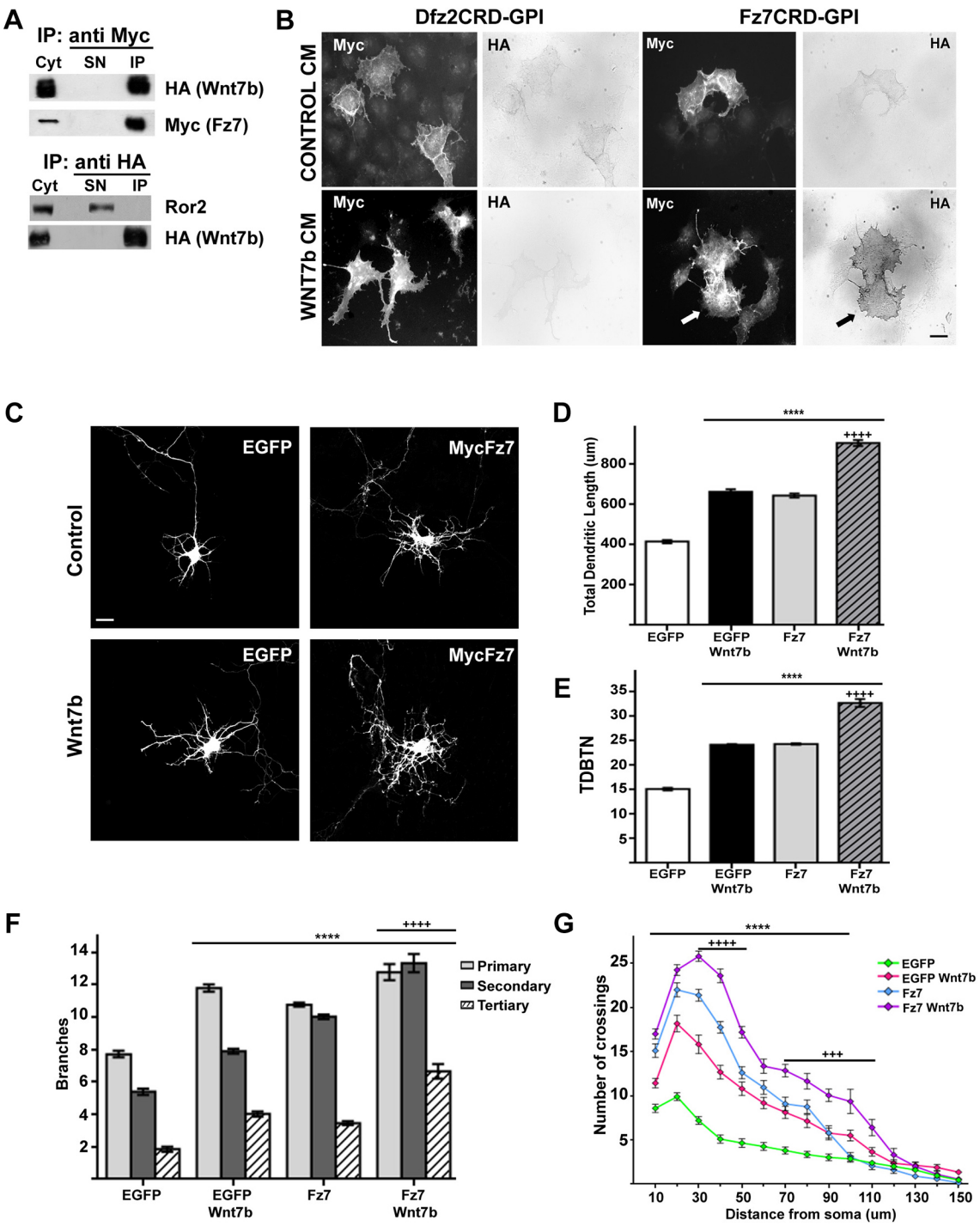

Fig. 2. Fz7 promotes dendrite development by binding to Wnt7b. (A) Immunoprecipitation experiments show that Fz7 forms a complex with Wnt7b in HEK293 cells. Pulldown assays were performed with anti-Myc or HA antibodies and probed with anti-HA, -Myc or -Ror2 antibodies. Immunoprecipitation shows that Wnt7b interacts with Fz7 but not Ror2. Cyt, cytosol; SN, supernatant after immunoprecipitation; IP, immunoprecipitate. (B) Wnt7b–HA binds (dark staining) to Myc–Fz7CRD-GPI- but not to Dfz2CRD–Myc–GPI-expressing Cos-7 cells. Arrows indicate the surface interaction between Wnt7b and Fz7; 25 cells per condition were analysed from three independent experiments. (C) Fz7 induces dendrite growth and increases branching complexity. Images show the morphology of cultured neurons at 3 DIV expressing EGFP or MycFz7 and exposed to either control or Wnt7b-conditioned medium for 20 h. Quantification shows the effect of Fz7 in the presence or absence of Wnt7b on total dendritic length (D), total dendritic branch tip number (TDBTN) (E), the number of primary, secondary and tertiary branches orders (F) and the number of intersections as determined by Sholl analysis (G). ****P<0.0001 compared to controls (EGFP), ^{++++}P<0.0001, ^{++}P<0.001, compared to EGFP+Wnt7b. Error bars represent mean±s.e.m. Scale bars: 10 µm.

Journal of Cell Science (2018) 131, jcs216101. doi:10.1242/jcs.216101

domain is required for signalling (Povelones and Nusse, 2005; Rodriguez et al., 2005; Sahores et al., 2010). Thus, to demonstrate whether Wnt7b binds to the CRD domain of Fz7, we performed surface binding assays after overexpressing the CRD domains of human Fz7 (Fz7CRD-GPI) or the *Drosophila* Frizzed 2 (Dfz2CRD-GPI) in Cos-7 cells (Fig. 2B). Transfected cells were then incubated with conditioned medium from either control or Wnt7b–HA-expressing cells. Immunocytochemical assays revealed that Wnt7b binds to cells expressing Fz7CRD-GPI (Fig. 2B, white arrow indicates Myc–Fz7CRD fluorescence and black arrow points to HA-Wnt7b phosphatase reaction). As expected, Wnt7b-HA did not interact with Dfz2CRD-GPI (Fig. 2B). Collectively, these findings demonstrate that Wnt7b binds to the Fz7 receptor.

Fz7 promotes dendrite development

The dendritic and growth cone distribution of Fz7, led us to test the hypothesis that Fz7 regulates dendrite development. As we previously showed for Wnt7b (Rosso et al., 2005), expression of Fz7 receptor induced a significant increase in the total dendritic length (Fig. 2C,D) and in the number of branches (the 'total dendritic branch tips number', denoted TDBTN) compared to EGFP-expressing control cells (Fig. 2C,E). The Fz7 effect on dendrites was enhanced when Fz7-overexpressing neurons were also stimulated by Wnt7b. Neurons displayed a significant increase (∼40%) in dendritic length and complexity (TDBTN) compared to what was seen for EGFP controls and Fz7 overexpression (Fig. 2C–E). Additionally, we analysed the complexity of dendritic trees by counting the number of primary, secondary and tertiary dendrites and applying Sholl analysis (Fig. 2F,G). Stimulation with Wnt7b and/or Fz7 expression increased the number of primary, secondary and tertiary branches orders compared to EGFP-expressing control neurons (Fig. 2F). Moreover, Fz7-expressing neurons stimulated by Wnt7b exhibited a further increase in dendritic complexity, which was evident by the increase in the number of higher branch orders compared to Wnt7b exposed or Fz7-expressing neurons (Fig. 2F,G). Wnt7b or Fz7 induced a significant increase in the number of intersections compared to EGFP controls, particularly within the ∼90 µm distance from the soma. In this context, we observed more marked effect on dendritic complexity in neurons expressing Fz7 and stimulated by Wnt7b. These neurons showed a further increase in total intersections until 110 µm of distance from the cell body than Fz7-expressing neurons (Fig. 2G). Taken together these findings demonstrate that Wnt7b and Fz7 receptor modulate the dendritic development and complexity of hippocampal neurons.

Fz7 promotes dendrite development by binding to Wnt7b

Considering that Wnt7b binds to Fz7 receptor, and that both molecules affect dendritic arborisation, we investigated whether Fz7 functions as a Wnt7b receptor during dendrite development by expressing the Fz7CRD, which binds to Wnt7b ligand and therefore blocks the activation of Fz7, or by silencing Fz7 with specific shRNA. First, we examined the efficiency of Fz7 silencing by expressing the Fz7 shRNA in 3DIV hippocampal neurons, using scrambled sequence shRNA (ssRNA) used as control (Fig. 3A). We observed that Fz7 shRNA induced an ∼50% decrease in the endogenous Fz7 level (Fig. 3A). Immunofluorescence images showed that the Wnt7b-mediated increase in dendritic length was blocked when neurons were exposed to the CRD domain of Fz7 (Fz7CRD) or when Fz7 was silenced (Fig. 3B–D). Similar results were obtained when we analysed the dendritic complexity, as Wnt7b-stimulated neurons elicited a marked increase in the TDBTN (∼60%) and in the number of primary, secondary and tertiary dendrites in respect to controls (Fig. 3C–E). However, this effect was abolished in Fz7CRD or Fz7 shRNA-expressing neurons. Interestingly, neurons expressing Fz7 shRNA and stimulated with exogenous Wnt7b had shorter and less-complex dendrites than EGFP controls, suggesting that Fz7 is required to maintain normal dendrite length and complexity (Fig. 3C–E; Fig. S1).

Sholl analysis revealed that Wnt7b stimulation induced a significant increase in the number of intersections until a distance of 90 µm from the soma, compared to EGFP-expressing cells as shown before (Fig. 2). In contrast, Wnt7b failed to increase the dendritic complexity in neurons expressing Fz7CRD or Fz7 shRNA, as the number of intersections decreased to control levels (Fig. 3F). These findings suggest that Fz7 is a receptor for Wnt7b during dendritic development.

Next, we performed a rescue assay to examine whether Fz7 overexpression rescues the Fz7 shRNA-induced dendritic defect. We observed that Fz7 shRNA led to defects in dendrite development as neurons have fewer and shorter dendrites (Fig. S1A–C). Expression of Fz7 cDNA in Fz7 shRNA-expressing pyramidal neurons rescued the dendritic defects as neurons had similar dendritic arbors to EGFP-expressing control cells (Fig. S1A–C). Importantly, no significant differences were observed between ssRNA- and EGFP-expressing neurons, therefore we used EGFP neurons as controls throughout the paper (Fig. S1D,E). Taken together, these findings demonstrate that Fz7 is required as a Wnt7b receptor to control dendrite formation and complexity in hippocampal neurons during dendritogenesis.

Fz7 signalling is required for functional dendritic development *in vivo*

To examine whether Fz7 signalling is critical for dendritogenesis in the intact developing brain, we decided to knockdown Fz7 at P0 rather using a Fz knockout model to restrict Fz7 manipulation to the period of dendritogenesis. Fz7 was knocked down by intraventricular injection of AAV1–Fz7 shRNA-mCherry in P0 newborn Thy1–GFP-expressing mice (Fig. 4A). Brain slices were subsequently labelled for mCherry and GFP to analyse dendritic complexity in the shRNA-expressing neurons in granule cells of the dentate gyrus (Fig. 4B). Importantly, neurons expressing Fz7 shRNA showed a marked defect on dendritic complexity (Fig. 4C). Quantification revealed a 50% reduction in dendritic length (Fig. 4D), and Sholl analysis showed a significant decrease in the dendritic complexity in Fz7 shRNA-expressing neurons compared to those expressing scrambled shRNA control (Fig. 4E). These results demonstrate that the Fz7 receptor is required for dendritogenesis in the intact hippocampus.

Fz7 signals through Dvl1 to modulate dendrite development

Activation of Fz receptors by binding of Wnt ligands typically results in the recruitment of the Dvl1 to the cell membrane (Axelrod et al., 1998; Umbhauer et al., 2000; Wong et al., 2003). This event can activate three different pathways: the Wnt/β-catenin pathway, the planar cell polarity (PCP) pathway or the Ca^{2+} pathway depending on the cellular process (Clevers and Nusse, 2012). We previously demonstrated that Wnt7b, through Dvl1, modulates dendrite formation and maturation by activating a non-canonical pathway in hippocampal neurons (Rosso et al., 2005). To examine whether Dvl1 is required for the Fz7 receptor to regulate dendritic arborisation we knocked down Dvl1 expression by using a specific

Journal of Cell Science (2018) 131, jcs216101. doi:10.1242/jcs.216101

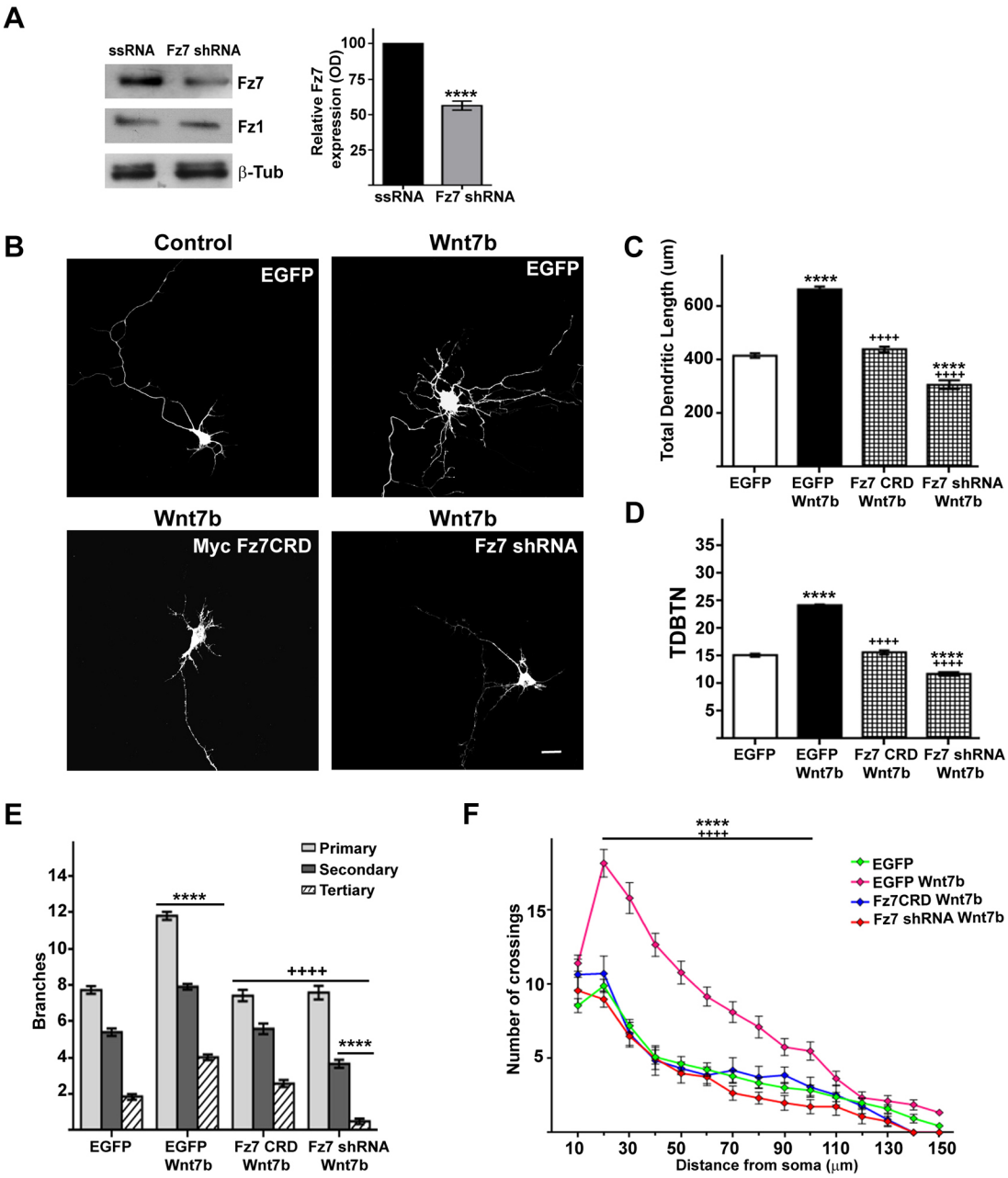

Fig. 3. Fz7 functions as Wnt7b receptor for dendritic development. (A) Western blots showing protein levels of Fz7 and Fz1 (as a specificity control) in neurons expressing Fz7 shRNA or the scrambled sequence RNA (ssRNA). β-tubulin was used as a loading control. The quantification on the right shows that we observed a substantial decrease in Fz7 expression in the shRNA-expressing cells. (B) Representative images from 3 DIV control or Wnt7b-stimulated neurons expressing EGFP, Myc–Fz7CRD or Fz7 shRNA. Quantifications show the impact of Fz7 on total dendritic length (C), TDBTN (D), the number of primary, secondary and tertiary dendrites (E) and number of crossings as determined by Sholl analysis (F), from control or Wnt7b-exposed neurons expressing the EGFP, Fz7CRD or Fz7 shRNA construct. $^{****}P<0.0001$ compared to control (ssRNA or EGFP), $^{++++}P<0.0001$ compared to EGFP+Wnt7b. Error bars represent mean ±s.e.m. Scale bar: 10 µm.

shRNA (Dvl1 shRNA) (Fig. 5). First, we analysed the efficiency of Dvl1 shRNA to downregulate the expression of HA-tagged Dvl1 in neurons and found that Dvl1 shRNA expression induced a decrease of 75% in neurons (Fig. 5A).

Next, we examined the impact of silenced Dvl1 on Fz7-expressing neurons. Fz7 overexpression led to a significant enhancement of total dendritic length and the number of branches when compared to control EGFP-expressing neurons. However, these effects were inhibited when Dvl1 was silenced, as neurons exhibited decreased dendritic length, defects in TDBTN and in the number of primary, secondary and tertiary dendrites (Fig. 5B–E). Consistent with these results, the dendritic complexity as obtained by Sholl analysis revealed a significant increase in the number of intersections for Fz7-expressing neurons within the ∼90 µm closest to the soma as compared to the number in control EGFP-expressing neurons. Similar results were obtained when neurons co-expressed Fz7 and the control ssRNA (data not shown). However, this increase was completely abolished when Dvl1 was silenced in Fz7-expressing neurons (Fig. 5F). Collectively, these findings suggest that Fz7 requires Dvl1 function to regulate dendrite morphogenesis.

Journal of Cell Science (2018) 131, jcs216101. doi:10.1242/jcs.216101

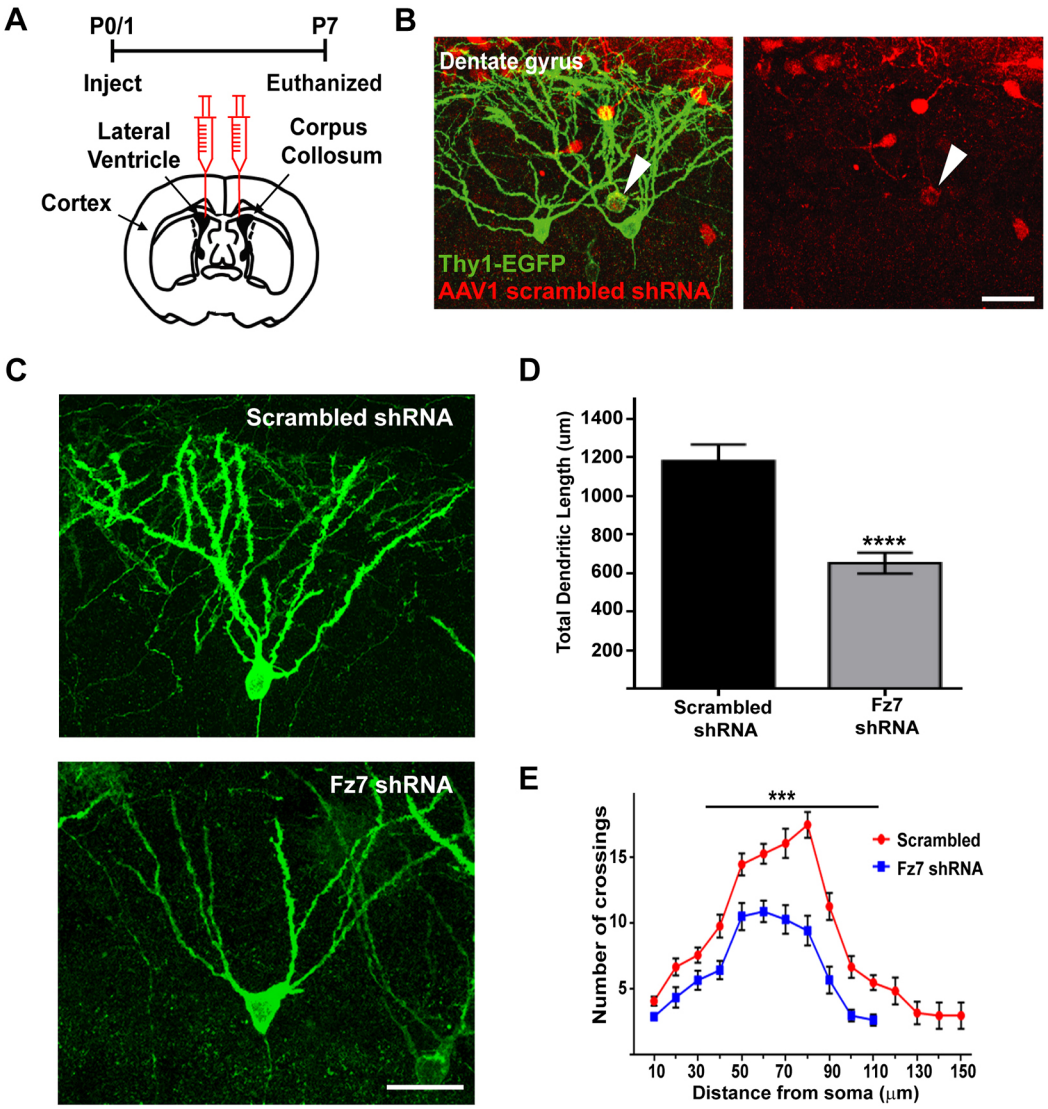

Fig. 4. Dendritogenesis requires Fz7 in the intact hippocampus. (A) Schematic of intracranial injection sites for AAV1 with scrambled or Fz7 shRNA coexpressing mCherry into the cerebral lateral ventricles of P0–P1 Thy1–EGFP mice. Mice were killed 7 days later. (B) Representative images of Thy1-expressing granule cells (green) in the dentate gyrus, which colocalised with AAV1 with scrambled shRNA (red; arrowhead). (C) Representative images from P7 mice expressing scrambled or Fz7 shRNA. Scale bar: 25 µm. Quantification of total dendritic length (D) and number of crossings as determined by Sholl analysis (E) comparing scrambled and Fz7 shRNA cells. ***P<0.001, ****P<0.0001 (n=12–13 cells from seven independent mice per condition). All error bars represent mean±s.e.m. Scale bars: 25 µm.

JNK functions downstream of Fz7 to modulate dendrite architecture

We previously demonstrated that Wnt7b modulates dendrite development through the JNK pathway (Rosso et al., 2005). In this study, we examined whether Wnt7b acts through Fz7 to activate JNK. Interestingly, our observations revealed that neurons expressing Fz7 displayed a higher level of phosphorylated (p-)JNK (active JNK) than controls, and that the increase was even higher in neurons also stimulated with Wnt7b (Fig. 6A). Importantly, expression of the Fz7CRD or Fz7 shRNA blocked the Wnt7b effect on JNK activity, suggesting that Wnt7b requires Fz7 to modulate JNK activation (Fig. 6B,C). Additionally, we analysed whether the Fz7 effect on dendrites requires JNK activation by blocking JNK with either a specific pharmacologic inhibitor (SP600125) or through the expression of JBD, a dominant-negative form of JNK (Dickens et al., 1997). Neurons expressing Fz7 and treated with the JNK inhibitor or co-expressing the JBD construct had shorter and less-complex dendritic arbors than did Fz7-expressing neurons (Fig. 6D). Quantitative analyses showed that inhibition of JNK or JBD expression significantly decreased total dendritic length (Fig. 6E), branch number (Fig. 6F), neurite orders (Fig. 6G) and the number of branch intersections (Fig. 6H). These findings suggest that Fz7 signals through JNK to regulate dendrite development.

Fz7 modulates dendrite development through CaMKII

A Wnt molecule that is highly similar to Wnt7b, Wnt7a, has been previously demonstrated to activate CaMKII on dendrites during synapse formation (Ciani et al., 2011). Furthermore, CaMKII is extensively involved in many neuronal events (developmental processes to plasticity) (Wu and Cline, 1998; Wayman et al., 2008). We therefore decided to examine the contribution of CaMKII to Wnt7b-mediated dendritic arborisation.

First, we examined whether Wnt7b, through Fz7, was able to modify the activity of CaMKII in dissociated hippocampal neurons.

Journal of Cell Science (2018) 131, jcs216101. doi:10.1242/jcs.216101

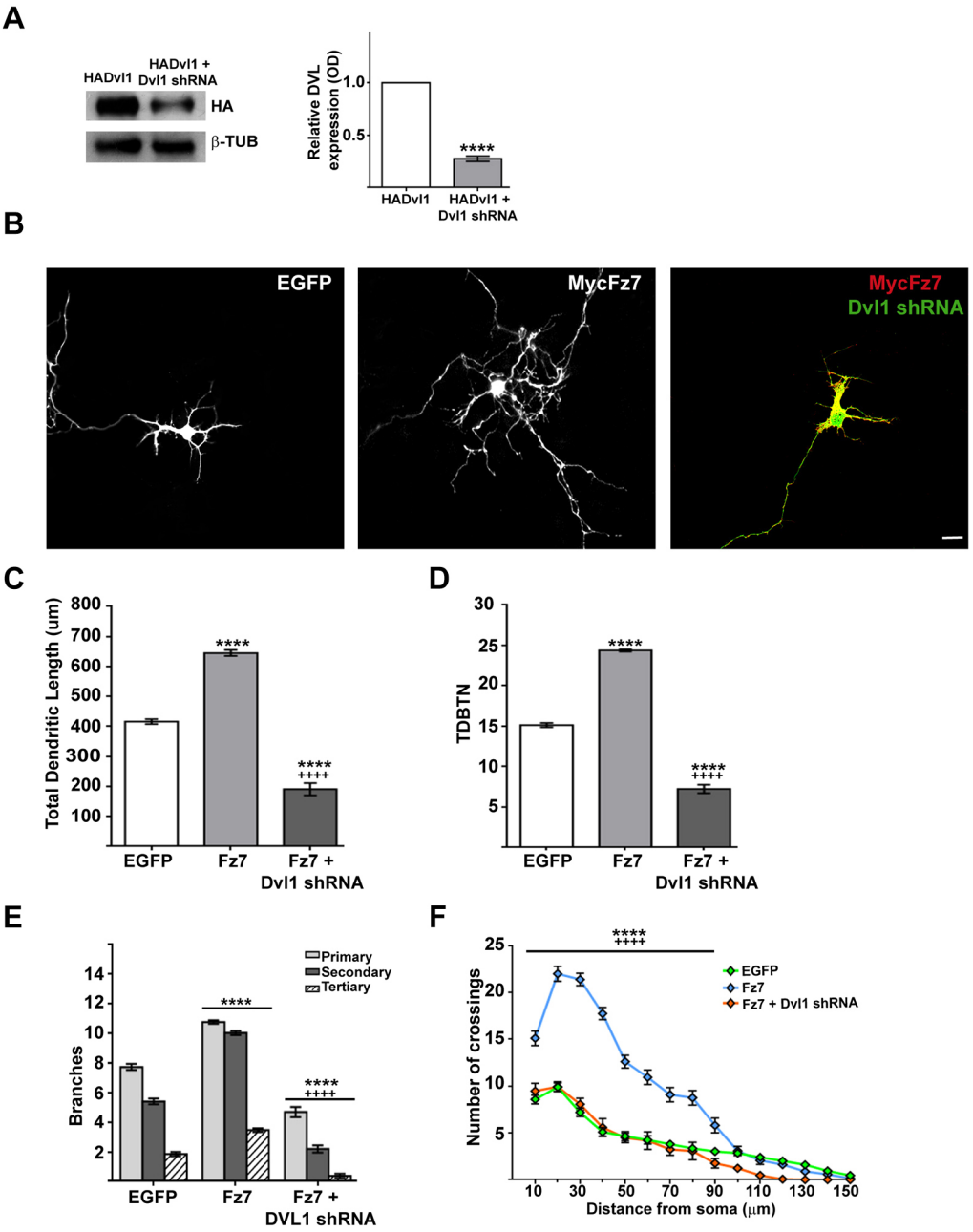

Fig. 5. Fz7 signals through Dvl1 to modulate dendrite development. (A) Western blots and quantification showing Dvl1 shRNA efficiency in Dvl1-expressing neurons. Relative optical density of Dvl1 expression. β-tubulin was used as loading control. ****P<0.0001 compared to HA–Dvl1-expressing cells. (B) Representative images from 3 DIV cultured neurons expressing EGFP, Myc–Fz7, or co-expressing Myc–Fz7 and Dvl1 shRNA. Yellow cells confirmed co-transfection of Myc–Fz7 (red) and Dvl1 shRNA (green). Quantitative analyses of total dendritic length (C), TDBTN (D), number of primary, secondary and tertiary branches (E) and the number of intersections as determined by Sholl analysis (F) from 3 DIV neurons under different experimental condition. ****P<0.0001 compared to control (EGFP), ^{++++}P<0.0001 compared to Fz7-expressing neurons. Error bars represent mean±s.e.m. Scale bar: 10 µm.

To analyse CaMKII activation, we measured the level of phosphorylated CaMKII (p-CaMKII) as a read-out of the CaMKII activity. Neurons exposed to Wnt7b or expressing Fz7 showed a marked increase in the level of p-CaMKII (~50%) compared to that in EGFP-expressing cells, whereas total CaMKII levels remained unchanged (Fig. 7A). Importantly, Fz7-expressing neurons challenged by Wnt7b showed a pronounced increase (~95%) in p-CaMKII compared to control EGFP-expressing neurons, which was significantly different from that seen in Fz7-expressing cells (~42%) (Fig. 7A). This Wnt7b–Fz7-mediated effect on CaMKII activity was blocked when neurons expressed the Fz7CRD or when Fz7 was silenced (Fz7 shRNA) (Fig. 7A). Thus, Fz7 activates endogenous CaMKII in hippocampal neurons during dendritogenesis.

To test whether the regulation of CaMKII activity by Fz7 is important for dendritic development and complexity, we blocked CaMKII either by silencing CaMKII with shRNA or by exposing neurons to the specific CaMKII-blocking peptide AIP (Ishida et al., 1995). Neurons expressing either Fz7 and CaMKII shRNA, or Fz7 and exposed to AIP had shorter and fewer branched dendrites compared to Fz7-expressing neurons (Fig. 7B). Quantification revealed that CaMKII shRNA expression or AIP treatment decreased dendritic length (Fig. 7C), decreased the TDBTN (Fig. 7D) and decreased the number of primary, secondary and tertiary branches (Fig. 7E). In addition, Sholl analysis showed a significant decrease in the number of intersections up to 90 µm from the soma in both Fz7 and CaMKII shRNA co-expressing neurons, and in Fz7-expressing neurons exposed to AIP treatment when compared to the number in Fz7-expressing cells (Fig. 7F). These results suggest that Fz7 regulates dendritic growth through activation of CaMKII.

Fz7 signalling to CaMKII requires Dvl1

To investigate the mechanism of action, we evaluated whether the downstream Fz7 effector Dvl1 can modulate dendritic architecture through CaMKII activation. First, we analysed the activation of

Journal of Cell Science (2018) 131, jcs216101. doi:10.1242/jcs.216101

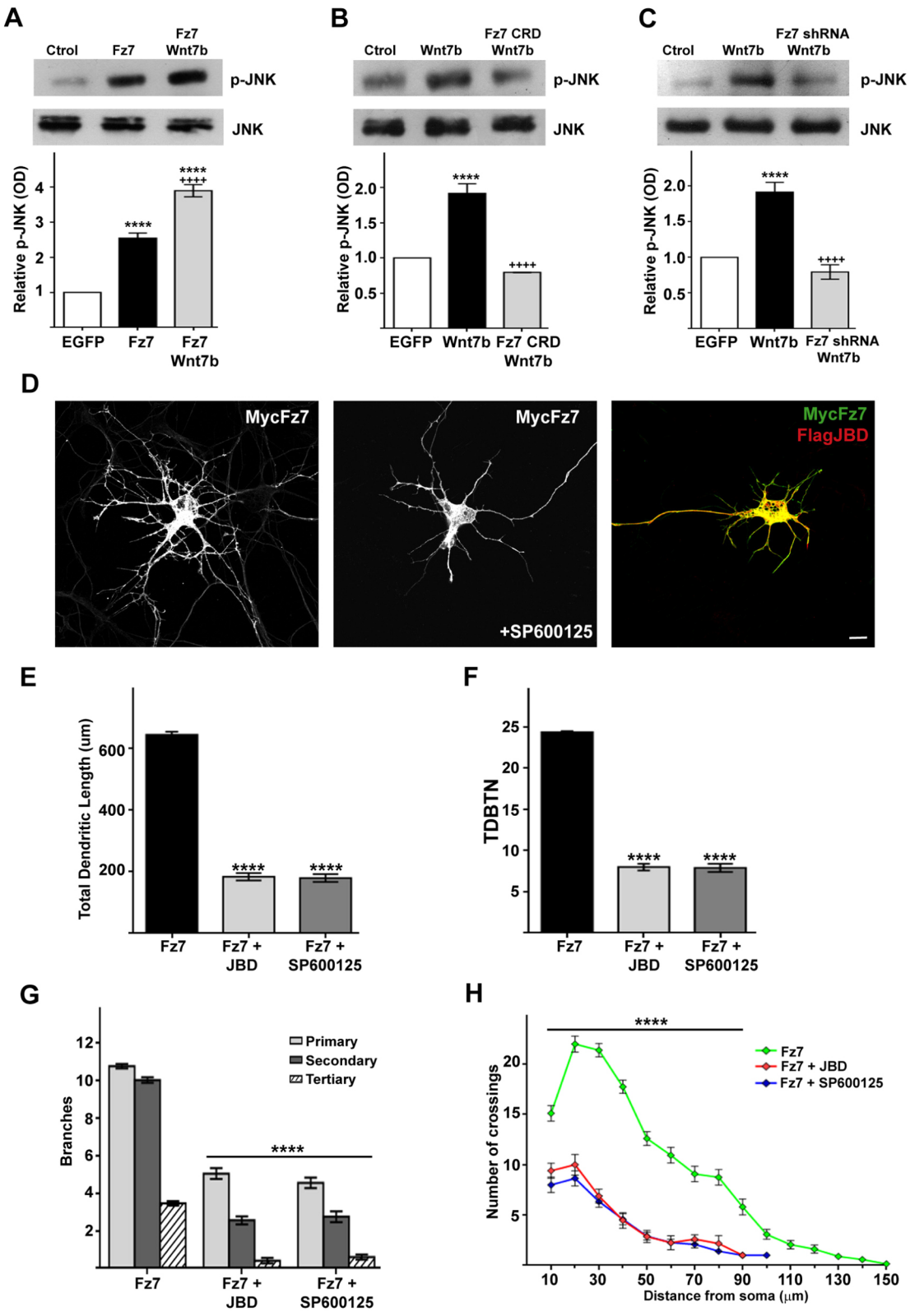

Fig. 6. Fz7 modulates dendritic architecture through activation of JNK. (A) JNK activity (p-JNK) in controls, Fz7-expressing neurons (Fz7) and Fz7-expressing neurons in the presence of Wnt7b-conditioned medium for 20 h. (B) Activation of JNK in controls, Wnt7b-stimulated neurons and Fz7CRD neurons exposed to Wnt7b. (C) JNK activity in controls, Wnt7b-stimulated neurons and in Fz7 shRNA-silenced neurons exposed to Wnt7b. Lower panels show the quantification of relative optical density of p-JNK. For each experiment, total JNK was used as loading control. ****P<0.0001 compared to control (EGFP), ^{++++}P<0.0001 compared to Wnt7b or Fz7 condition. (D) Representative images from 3 DIV cultured neurons expressing Myc–Fz7 either in control medium or treated with SP600125, or co-expressing Myc–Fz7 and Flag–JBD. Quantitative analysis shows total dendritic length (E), TDBTN (F), the number of primary, secondary and tertiary dendrites (G) and the number of crossings as determined by Sholl analysis (H). ****P<0.0001 compared to Fz7-expressing cells. Error bars represent mean±s.e.m. Scale bar: 10 µm.

Journal of Cell Science

Journal of Cell Science (2018) 131, jcs216101. doi:10.1242/jcs.216101

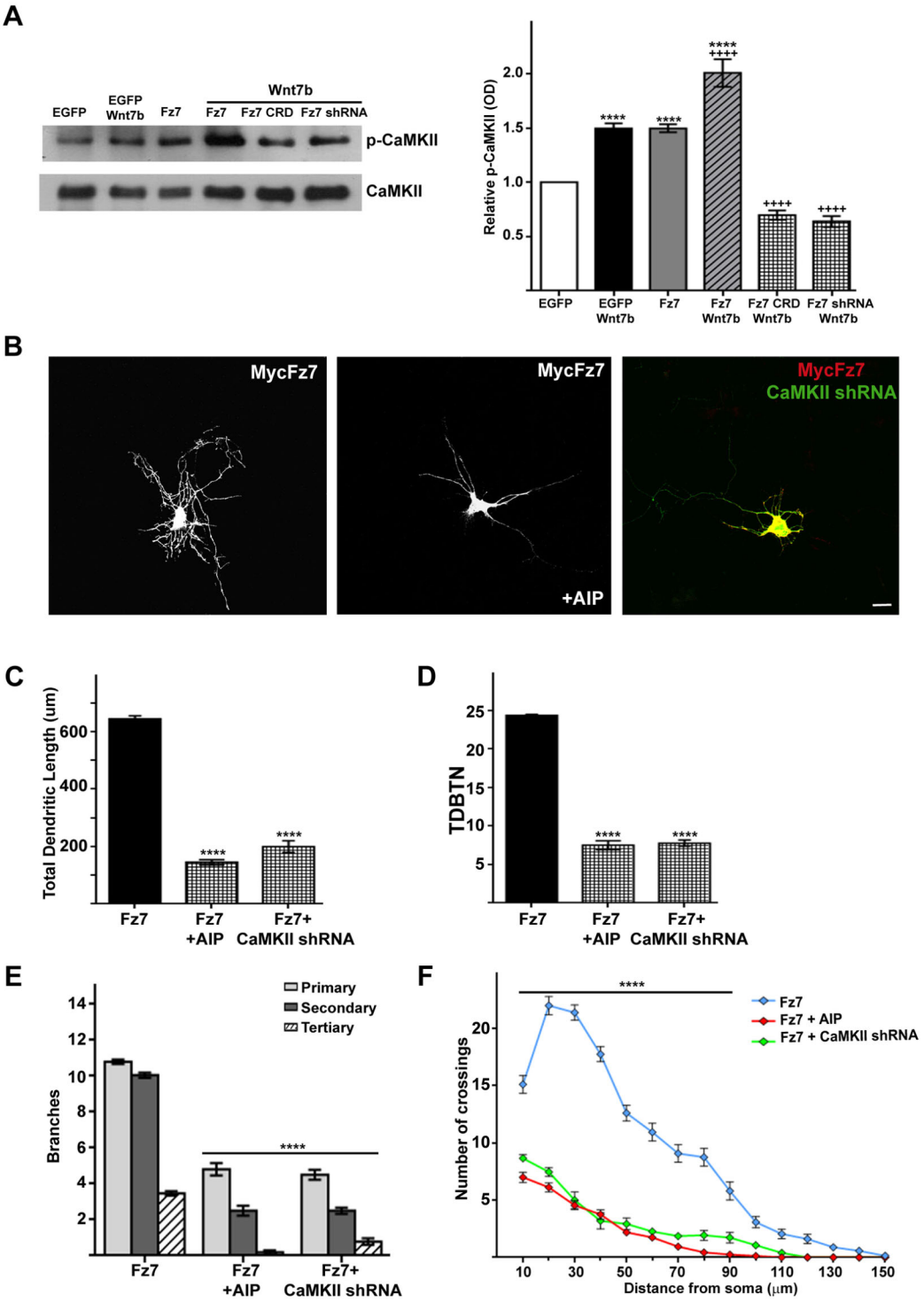

Fig. 7. Fz7 requires CaMKII to modulate dendritic arborisation. (A) Western blots showing the CaMKII activity (p-CaMKII) in control neurons (EGFP), Wnt7b-stimulated neurons (EGFP Wnt7b), Fz7-expressing neurons with or without Wnt7b, and in Fz7CRD- or Fz7 shRNA-expressing cells exposed to Wnt7b-conditioned medium for 20 h. Total CaMKII was used as loading control. In the right panel, the quantification shows the relative optical density (OD) of p-CaMKII for each condition. ****P<0.0001 compared to control (EGFP), ^{++++}P<0.0001 compared to EGFP–Wnt7b- and Fz7-expressing neurons. (B) Representative images from 3 DIV cultured neurons expressing Myc–Fz7, or co-expressing Myc–Fz7 and CaMKII shRNA; in the middle panel Fz7-expressing cells were treated with AIP (a CaMKII inhibitor). Immunostaining was performed with antibodies against Myc or GFP (for the CaMKII shRNA condition). Quantitative analysis shows total dendritic length (C), the TDBTN (D), the number of primary, secondary and tertiary dendrites (E) and the number of crossing as determined by Sholl analysis (F). ****P<0.0001 compared to Fz7-expressing cells. Error bars represent mean±s.e.m. Scale bar: 10 µm.

CaMKII in Dvl1-expressing neurons. Dvl1-expressing hippocampal neurons showed an increase (~50%) in the level of p-CaMKII compared to EGFP controls, whereas the total CaMKII expression remained unchanged (Fig. 8A). Next, we investigated whether Dvl1 requires CaMKII activation to modulate dendritic morphology by blocking CaMKII in Dvl1-expressing neurons by

Journal of Cell Science (2018) 131, jcs216101. doi:10.1242/jcs.216101

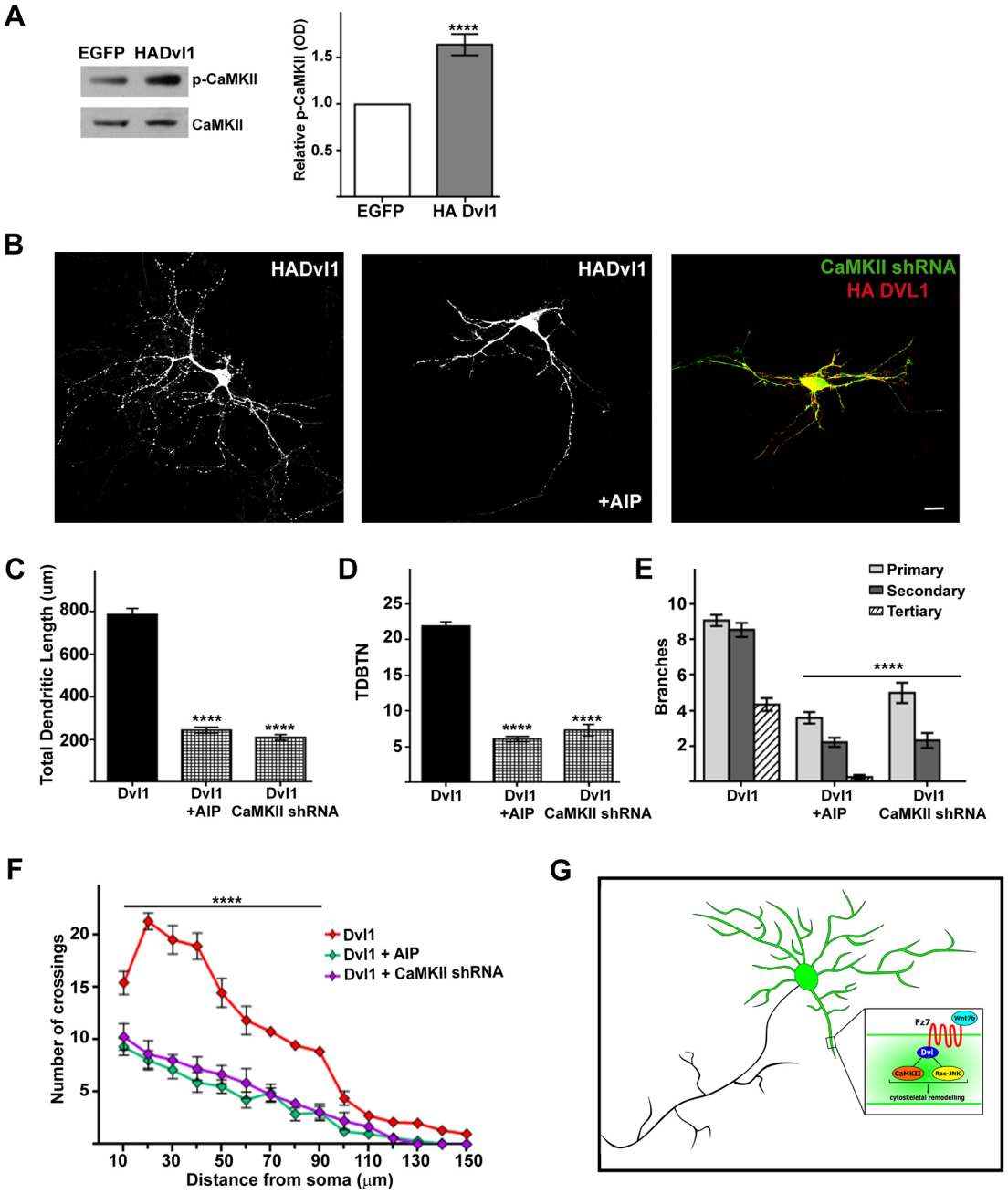

Fig. 8. Dvl1 dendritogenic effect is mediated by CaMKII. (A) Western blot showing CaMKII activity levels (p-CaMKII) in Dvl1-expressing neurons. Total CaMKII was used as loading control. The quantification shows the relative optical density (OD) of p-CaMKII. ****P<0.0001 compared to EGFP neurons. (B) Confocal images from 3 DIV cultured neurons expressing HA–Dvl1, or co-expressing HA–Dvl1 and CaMKII shRNA. Middle panel, HA–Dvl1-expressing cells were treated with AIP inhibitor. Quantification of total dendritic length (C), the TDBTN (D), the number of primary, secondary and tertiary dendritic branches (E) and the number of crossings as determined by Sholl analysis (F). ****P<0.0001 compared to Dvl1-expressing cells. Error bars represent mean±s.e.m. Scale bar: 10 µm. (G) Scheme showing that Wnt7b, through Fz7 and Dvl1, activates non-canonical CaMKII- and JNK-mediated pathways. This activation leads to changes in the cytoskeleton organisation, affecting dendrite growth and complexity. Effectors from both non-canonical pathways may affect microtubule and actin dynamics, modifying dendrite architecture.

using the AIP peptide or expressing the CaMKII shRNA. Although Dvl1-expressing neurons developed an elaborated dendritic tree, with long and highly branched dendrites, inhibition of CAMKII by means of AIP inhibitor or expression of CaMKII shRNA resulted in shorter and very poorly branched dendrites (Fig. 8B). Quantification revealed the effect of AIP or expression of CaMKII shRNA on Dvl1-mediated dendritic length (Fig. 8C), TDBTN (Fig. 8D) and the number of secondary and tertiary order branches (Fig. 8E). Furthermore, the dendritic complexity was reduced, as Sholl analysis revealed a marked decrease in the number of intersections up to 90 µm from the cell soma compared to that seen in Dvl1-expressing neurons (Fig. 8F). These findings suggest that Dvl1 requires CaMKII activation to modulate dendritic complexity.

DISCUSSION

The mechanisms controlling the formation and maturation of dendrites have been studied in detail, mainly focusing on the

extracellular factors and signalling pathways involved in dendrite remodelling and maturation (Van Aelst and Cline, 2004; Salama-Cohen et al., 2006; Kulkarni and Firestein, 2012). However, the specific receptors required for regulating these processes in the mammalian system remain poorly characterised.

Wnt proteins, through their specific receptors modulate neuronal functioning by regulating axon guidance (Lyuksyutova et al., 2003), dendrite development (Rosso et al., 2005) and synapse assembly (Varela-Nallar et al., 2009; Sahores et al., 2010; Ciani et al., 2011). Reports have demonstrated the role of Frizzled receptors in neurogenesis and differentiation of immature neurons (Armstrong et al., 2011; Hua et al., 2014; Marcos et al., 2015; Morello et al., 2015; Mardones et al., 2016). In addition, other studies have demonstrated a role for Fz proteins in synapse formation. For example, Fz1 mediates synaptic differentiation (Varela-Nallar et al., 2009), Fz5 regulated Wnt7a-mediated synaptic assembly in hippocampal neurons (Sahores et al., 2010) and Fz4 participates in the maintenance of the cerebellum structure and its connectivity (Wang et al., 2001). These studies suggest that Fz receptors play an essential role in neuronal connectivity. However, little is known about the specificity of Wnt–Fz interaction and its function on dendritic development.

Studies on Fz7 reveal a role for this Wnt receptor in several cellular processes. Analyses of the Fz7-null mice have shown that they have no significant defects during early embryonic development; however, a marked phenotype is observed in $Fz2^{-/-}$; $Fz7^{-/-}$ double mutants, characterised by heart abnormalities and altered neural tube closure (Yu et al., 2012). In addition, we recently demonstrated that loss of function of Fz7 leads to defects in synaptic spine plasticity (McLeod et al., 2018). Indeed, Wnt7a–Fz7 signalling is required for glutamatergic AMPA receptor localisation and long-term potentiation (LTP)-mediated spine plasticity (McLeod et al., 2018). In the current study, we demonstrate that Fz7 also regulates dendrite formation and complexity.

Here, we report a novel role for Fz7 on dendrite architecture and maturation. We have previously demonstrated that Wnt7b regulates dendrite development and complexity through a non-canonical pathway (Rosso et al., 2005). However, its specific membrane receptor had not previously been identified. In this work, we showed that Fz7 is developmentally expressed in the hippocampus and in hippocampal pyramidal neurons, and its expression increases during dendrite formation and maturation. Importantly, Fz7 localises along the dendrites and their growth cones, suggesting a role in dendrite development. A previous study showed that the expression of Fz7 in the hippocampus decreases during development and almost disappears after P10 (Varela-Nallar et al., 2012). However, endogenous Fz7 levels increase during development, concurrently with dendrite maturation, reaching the highest level at the adult stage. This apparent discrepancy could be due to specificity and quality of the commercial antibodies for Fz7. Our experiments show that the anti-Fz7 antibody is specific as Fz7 shRNA results in a substantial decrease in the levels of endogenous Fz7 protein.

Our work demonstrates that Fz7 promotes dendrite morphogenesis and functions as a Wnt7b receptor during this process. Several observations led us to conclude this. Firstly, Wnt7b and Fz7 are both expressed in the hippocampus during dendritogenesis (Shimogori et al., 2004; Rosso et al., 2005). Furthermore, Fz7 protein is present along dendrites as they extend. Secondly, Fz7 co-immunoprecipitates with Wnt7b, and Wnt7b binds to Fz7 in cultured cells. Thirdly, Wnt7b requires Fz7 to modulate dendrite formation and complexity in dissociated hippocampal neurons, as knockdown or blockage of Fz7 abolishes the Wnt7b effects on dendrites. Fourthly, *in vivo* studies show that suppression of Fz7 expression in mice leads to marked defects on dendritic morphology, as neurons develop short and unbranched dendrites. These results strongly support the idea that Fz7 functions as the Wnt7b receptor to regulate dendrite morphogenesis in the developing hippocampus.

How does Wnt7b–Fz7 regulate dendritic development? Wnt7b signals through Fz7 receptor to activate the non-canonical Ca^{2+} pathway to modulate dendrite complexity. The role of CaMKII on neuronal development and function has been extensively examined in the past two decades (Wu and Cline, 1998; Wen et al., 2004; Wayman et al., 2008). Ca^{2+}-sensitive enzymes such as CaMKII control neuronal growth and synaptogenesis, as its expression and subcellular localisation are developmentally regulated (Kelly and Vernon, 1985; Scheetz et al., 1996; Wu and Cline, 1998). CaMKII has a positive function on filopodia extension and dendrite development through a direct interaction with cytoskeletal actin (Fink et al., 2003). Furthermore, Map2, a dendritic microtubule-associated protein, can be phosphorylated by CaMKII affecting dendritic architecture (Friedrich and Aszódi, 1991; Díez-Guerra and Avila, 1993). Thus, changes in CaMKII activity modulate the Map2–microtubule interaction, affecting dendrite stability and morphology (Vaillant et al., 2002). In our work, Wnt7b–Fz7, through Dvl1, activated CaMKII and that activation was abolished when Fz7 was blocked. Changes in CaMKII activity may affect the stability of dendritic microtubules. The regulation of Map2 phosphorylation and microtubule stability by Wnt7b–Fz7 signalling remains to be analysed.

Previously, we identified Rac1 and JNK as critical downstream effectors of Wnt7b-Dvl1-mediated dendritogenesis (Rosso et al., 2005). In the present work, we showed that JNK is also a downstream effector of Fz7 receptor. Based on our new results, both Wnt pathways, the PCP and the Ca^{2+}-signalling pathway, are involved in Wnt7b/Fz7-mediated dendritic development. Activation of both cascades may modulate the function of key players that control the organization of dendritic cytoskeleton (Fig. 8G). Further studies are required to determine whether these two pathways converge or act independently to promote dendritic development. In conclusion, our results demonstrate a novel role of Fz7 in dendritic development. Our findings describe a signalling pathway that requires Wnt7b, its receptor Fz7 and the scaffold protein Dvl1 to coactivate CaMKII and JNK, resulting in the formation of complex dendrites, which are crucial for neuronal integration.

MATERIALS AND METHODS

Animals

Wistar rats were group housed in a climate controlled room with a 12-h-light–12-h-dark cycle, food and water were provided *ad libitum*. All animal procedures were performed following approved protocols of the National Institutes of Health Guide for the Care and Use of Laboratory Animals. Approval to conduct the study was granted by the Animal Care and Ethics Committee of the School of Biochemical and Pharmaceutical Sciences, National University of Rosario, Argentina.

C57BL/6J Thy1-EGFP mice were housed at University College London, UK, with a 112-h-light–12-h-dark cycle, food and water were provided *ad libitum*. All experiments and procedures were performed according to the Animals Scientific Procedures Act UK (1986).

Neuronal culture and transfection

Primary cultures of rat hippocampal pyramidal cells were prepared as previously described (Rosso et al., 2004). Whole brains were obtained from embryonic day 19 (E19) rat embryos and dissected in chilled Hank's balanced salt solution (HBSS) (Gibco, Grand Island, NY) to isolate the hippocampi. These were incubated with HBSS containing 0.25% trypsin,

Journal of Cell Science (2018) 131, jcs216101. doi:10.1242/jcs.216101

and cells were mechanically dissociated in DMEM10 (DMEM with 10% horse serum; Gibco) and plated onto coverslips coated with poly-L-lysine (1 mg/ml, Sigma-Aldrich, St Louis, MO) at low density (7.5×10^4 cells/cm^2) or high density (1×10^5 cells/cm^2), depending on the experiment. Neurons were incubated at 37°C in a humidified atmosphere with 5% CO_2 in DMEM10 and after 2 h, medium was replaced with Neurobasal medium, supplemented with 2% B27 (Gibco).

To analyse the spatial and temporal distribution of Fz7, low-density cultures were fixed at 1, 2 and 4 DIV according to the cytoskeleton-stabilising procedure described by Nakata and Hirokawa (Nakata and Hirokawa, 1987), whereas high-density cultures were carried out to evaluate Fz7 expression at 2, 6 and 10 DIV by western blotting.

Neuronal transfections were performed on high-density cultures at 2 DIV using Lipofectamine 2000 (Life Technologies, Carlsbad, CA, USA) according to the manufacturer's protocol, and either cell fixation or protein extraction were carried out at 3 DIV. For stimulation assays, Wnt7b-conditioned medium was obtained from stably transfected Rat1B cells (Rosso et al., 2005). Different DNA constructs were used: EGFP, Fz7 and Fz7 CRD tagged with Myc, Dvl1 tagged with HA, and JBD tagged with Flag. At 2 h after transfection, neurons were treated with conditioned medium and cultured for 15 h further. For CaMKII and JNK inhibition experiments, 1 µM autocamtide-2-related inhibitory peptide (AIP, Sigma-Aldrich), or 10 µM SP600125 (Abcam, Cambridge, MA), respectively, was added at 2 h post transfection and left overnight. Cells were fixed for 20 min at room temperature with 4% (w/v) paraformaldehyde in phosphate-buffered saline (PBS) containing 4% (w/v) sucrose (PFA/S).

A MaxiPrep endotoxin-free kit (Qiagen, Hilden, Germany) was used to obtain plasmids for neuronal transfection. cDNAs encoding shRNAs were inserted into a pSuper. neo+GFP vector (pSuper RNAi System; OligoEngine, Seattle, WA) with target sequences as follows: Fz7 shRNA (5′-GCTTCTTCTTATGCTCTAT-3′), Dvl1 shRNA (5′-TCCGGGACCG-CATGTGGCT-3′), CaMKII shRNA (5′-ACTGTATCCAGCAGATCCT-3′) and scrambled sequence ssRNA (5′-GCACTTCATGCCACTAGAT-3′), as described by Coullery et al. (Coullery et al., 2016).

In vivo expression of Fz7 shRNA

Thy1-EGFP mice (P0–P1) were anaesthetised with isoflurane until they ceased to move. AAV1 packaged with scrambled or Fz7 shRNA (expressing mCherry) was then injected bilaterally into the ventricles using a 50 µl Hamilton syringe attached to a 33-gauge needle (Hamilton, 65460-16). The injection site was located at two-fifths of the distance between each eye and the Lambda point as previously described (Kim et al., 2013). The needle was inserted ∼1 mm in depth within the skull and 3 µl of virus (2×10^8 virus particles/hemisphere) was injected. Pups were then placed on a warming pad to recover before being transferred back to their mother. Animals were euthanised by a Schedule 1 procedure under the Home Office Animals (Scientific Procedures) Act 1986 at 1-week following the injection.

Immunofluorescence and image acquisition

Brains from the pups were fixed overnight at 4°C with 4% paraformaldehyde in PBS, washed twice with PBS, transferred to 30% sucrose in PBS then frozen with isopentane on dry ice. Subsequently, 50 µm sections were cut on a cryostat then stored in ethylene glycol-based cryoprotectant (30% glycerol, 30% ethylene glycol in 0.1 M sodium/potassium phosphate buffer, pH 7.4) before immunostaining was commenced. Brain sections were washed twice with PBS and then incubated in blocking solution (10% donkey serum and 0.5% v/v Triton X-100 in PBS) for 4–6 h at room temperature. Next, sections were incubated with primary anti-GFP (1:500, chicken, cat no. 06-896, Millipore); to label dendritic processes, and anti-mCherry (1:1000, rabbit, cat no. ab167453, Abcam); to identify infected cells overnight at 4°C. Following three washes in PBS, Alexa Fluor 488- and 568-conjugated secondary antibodies were applied for 3 h at room temperature. Sections were washed a further three times in PBS, incubated with Hoechst 33342 for 5 min and finally mounted in Fluoromount-G (SouthernBiotech). Image stacks of granule cells in the dentate gyrus were captured on a Leica SP8 confocal microscope. Images were taken using a 40× oil objective, with 1024×1024 image resolution and a *z*-step of 0.5 µm. A total of 13–15 cells from seven independent mice per condition were acquired.

For dissociated neuronal assays, hippocampal pyramidal neurons were permeabilised with 0.2% Triton X-100 in PBS, and blocking was performed with 5% bovine serum albumin (BSA). Primary antibodies were prepared in 1% BSA and sample were incubated with primary antibody at 4°C overnight and with secondary antibodies at room temperature for 1 h. Primary antibodies used were: anti-class III-β-tubulin (1:5000, rabbit, cat. no. T2200, Sigma-Aldrich), anti-Fz7 (1:50, rabbit, cat. no. 06-1063, Millipore), anti-Map2 (clone AP-20, 1:450, mouse, cat. no. M1406, Sigma-Aldrich), anti-Myc (1:3000, mouse, cat. no. m4439, Sigma-Aldrich), anti-Myc (1:3000, rabbit, cat. no. SAB4300318, Sigma-Aldrich), anti-Tau-1 (1:600, mouse, clone Tau1, cat. no. MAB3420, Chemicon International), anti-HA (1:3000, rat, cat. no. 11867423001, Roche, Mannheim, Germany), anti-Flag (1:3000, mouse, cat. no. F3165, Sigma-Aldrich), anti-Tyr-Tubulin (1:2000, rat, cat. No. ab6160, Abcam). Secondary antibodies were: Alexa Fluor 546-conjugated anti-mouse-IgG, anti-rabbit-IgG or anti-rat-IgG, Alexa Fluor 488-conjugated anti-mouse-IgG, anti-rabbit-IgG or anti-rat-IgG, and Alexa Fluor 647-conjugated anti-mouse-IgG (all 1:600, Life Technologies, Eugene, OR). Images were captured with a Zeiss LSM880 spectral confocal microscope using a ZEN Lite 2012 system (blue edition). Images were taken using a 60× oil objective, with 1024×1024 image resolution. A total of 40–50 cells per condition were analysed from three independent experiments. Morphometrics analyses were performed using ImageJ software with the following plugins: NeuronJ to trace and measure dendrite length (µm) and number of branching (Meijering et al., 2004), and Sholl analysis to study the complexity of the dendritic arborisation (Ferreira et al., 2014). Measurements were conducted with researchers who were blind to the experimental conditions.

Wnt–receptor binding assay

Cos-7 cells were transfected with CRD domain of mouse Fz7 or *Drosophila* Dfz2, both containing a glycosyl-phosphatidylinositol (GPI) sequence (Fz7CRD-myc-GPI and Dfz2CRD-myc-GPI) (Hsieh et al., 1999). Transfected Cos-7 cells were incubated for 1 h at room temperature with control or Wnt7b–HA-conditioned medium obtained from stably transfected Rat1b cells. Subsequently, cells were fixed with 4% PFA/S, and incubated with primary antibodies against HA and Myc followed by incubation with alkaline phosphatase (AP)-conjugated antibodies (Amersham, Protran Premium, GE Healthcare, Little Chalfont, Buckinghamshire, UK) and Alexa Fluor 488-conjugated secondary antibodies (Molecular Probes). AP staining was developed according to the manufacturer's protocol (Amersham, Protran Premium, GE Healthcare, Little Chalfont, Buckinghamshire, UK). A total of 20–30 cells per condition were analysed from three independent experiments.

Immunoprecipitation experiments

HEK293 cell lines were co-transfected with Wnt7b-HA and Fz7-Myc plasmids and lysed 20 h after transfection in RIPA buffer at 4°C (Coullery et al., 2016). To carry out the assay, 400 µg of total protein were incubated overnight at 4°C with anti-HA antibody and protein A-Sepharose beads (Sigma, Saint Louis, MO, USA). Samples were analysed by Western blot using antibody against Myc and HA tags. Additionally, we probed whether Wnt7b interacts with endogenous Ror2, another receptor for Wnt proteins. Results were obtained from 3 independent experiments for each condition.

Hippocampal homogenates

Hippocampal homogenates were obtained from Wistar rats at different time points, starting at embryonic day 19 (E19) followed by postnatal days 0, 7, 14, 28 (P0-P28), to finish at adult stage. Whole brains were dissected, and hippocampi were isolated from both hemispheres, then homogenised on ice with RIPA buffer and kept chilled for 15 min. Finally they were centrifuged at 4°C and 15,000× ***g*** for 5 min and supernatant was recovered.

Electrophoresis and western blotting

E19 rat embryos hippocampal neurons were cultured as described previously, treated according to each experiment, and, at the corresponding time, cells were lysed with RIPA buffer plus proteases and phosphatases inhibitors, as previously reported (Coullery et al., 2016). For all experiments, membrane blocking was performed with 3% BSA, except

for HA and Myc detection where 5% milk was used. Primary antibodies were incubated at 4°C, overnight in 1% milk: anti-class III-β-tubulin III (1:10,000, rabbit, cat. no. T2200, Sigma-Aldrich), anti-HA (1:2000, rat, cat. no. 11867423001, Roche), anti-Myc (1:3000, mouse, cat. no. SAB1305535, Sigma-Aldrich), anti-phospho-SAPK/JNK (Thr183/Tyr185) (1:1500, rabbit, cat. no. 4668, Cell Signaling, Danvers, MA) or in 1% BSA: anti-Fz7 (1:2000, rabbit, cat. no. 06-1063, Millipore), anti-phospho-CaMKII^{Thr286} (1:1500, rabbit, cat. no. 3361, Cell Signaling), anti-pan-CaMKII (1:1500, rabbit, cat. no. 3362, Cell Signaling). All secondary antibodies (HRP-conjugated) were incubated at room temperature for 1 h in 0.2% milk: anti-rabbit-IgG (1:2000, Biorad, Hercules, CA, USA), anti-mouse-IgG (1:3000, Biorad, Hercules, CA, USA) and anti-rat-IgG (1:3000, Roche, Mannheim, Germany). Chemiluminescence was used as a detection method and membranes were exposed to X-ray films. Band optical density was measured with ImageJ software. All experiments were performed at least three times.

Statistical analysis

All graphs and statistical analyses were performed using GraphPad Prism software. Results correspond to the mean±s.e.m. Normally distributed data were analysed using either a Student's test or ANOVA with Tukey's post-hoc test for multiple comparisons. Statistical significance was labelled as $^{**}P<0.05$, $^{***}P<0.001$ and $^{****}P<0.0001$.

Acknowledgements

We are grateful to Rodrigo Vena for technical assistance with the confocal microscopy.

Competing interests

The authors declare no competing or financial interests.

Author contributions

Methodology: M.E.F., M.E.B., F.M., M.P., R.C., I.C., S.B.R.; Formal analysis: M.E.F., S.B.R.; Investigation: M.E.F., M.E.B., F.M., M.P., R.C., I.C., S.B.R.; Writing - original draft: M.E.F., F.M., M.P., P.C.S., S.B.R.; Writing - review & editing: F.M., M.P., P.C.S., S.B.R.; Supervision: S.B.R.; Funding acquisition: P.C.S., S.B.R.

Funding

This work was supported by grants from the Agencia Nacional de Promoción Científica y Tecnológica (ANPCyT-FONCyT) (PICT 2014-1326) to S.B.R., Consejo Nacional de Investigaciones Científicas y Técnicas (CONICET) (PIP 0947) to S.B.R., and Universidad Nacional de Rosario (UNR BIO 382) to S.B.R., Argentina, and by the Medical Research Council and Alzheimer's Research UK for P.C.S.

Supplementary information

Supplementary information available online at
http://jcs.biologists.org/lookup/doi/10.1242/jcs.216101.supplemental

References

Angers, S. and Moon, R. T. (2009). Proximal events in Wnt signal transduction. *Nat. Rev. Mol. Cell Biol.* **10**, 468-477.

Armstrong, A., Ryu, Y. K., Chieco, D. and Kuruvilla, R. (2011). Frizzled3 is required for neurogenesis and target innervation during sympathetic nervous system development. *J. Neurosci.* **31**, 2371-2381.

Axelrod, J. D., Miller, J. R., Shulman, J. M., Moon, R. T. and Perrimon, N. (1998). Differential recruitment of Dishevelled provides signaling specificity in the planar cell polarity and Wingless signaling pathways. *Genes Dev.* **12**, 2610-2622.

Baj, G., Pinhero, V., Vaghi, V. and Tongiorgi, E. (2016). Signaling pathways controlling activity-dependent local translation of BDNF and their localization in dendritic arbors. *J. Cell Sci.* **129**, 2852-2864.

Ciani, L., Boyle, K. A., Dickins, E., Sahores, M., Anane, D., Lopes, D. M., Gibb, A. J. and Salinas, P. C. (2011). Wnt7a signaling promotes dendritic spine growth and synaptic strength through Ca(2)(+)/Calmodulin-dependent protein kinase II. *Proc. Natl. Acad. Sci. USA* **108**, 10732-10737.

Clark, C. E. J., Richards, L. J., Stacker, S. A. and Cooper, H. M. (2014). Wnt5a induces Ryk-dependent and -independent effects on callosal axon and dendrite growth. *Growth Factors* **32**, 11-17.

Clevers, H. and Nusse, R. (2012). Wnt/beta-catenin signaling and disease. *Cell* **149**, 1192-1205.

Conde, C. and Cáceres, A. (2009). Microtubule assembly, organization and dynamics in axons and dendrites. *Nat. Rev. Neurosci.* **10**, 319-332.

Coullery, R. P., Ferrari, M. E. and Rosso, S. B. (2016). Neuronal development and axon growth are altered by glyphosate through a WNT non-canonical signaling pathway. *Neurotoxicology* **52**, 150-161.

Dickens, M., Rogers, J. S., Cavanagh, J., Raitano, A., Xia, Z., Halpern, J. R., Greenberg, M. E., Sawyers, C. L. and Davis, R. J. (1997). A cytoplasmic inhibitor of the JNK signal transduction pathway. *Science* **277**, 693-696.

Díez-Guerra, F. J. and Avila, J. (1993). MAP2 phosphorylation parallels dendrite arborization in hippocampal neurones in culture. *Neuroreport* **4**, 419-422.

Fenstermaker, V., Chen, Y., Ghosh, A. and Yuste, R. (2004). Regulation of dendritic length and branching by semaphorin 3A. *J. Neurobiol.* **58**, 403-412.

Ferreira, T. A., Blackman, A. V., Oyrer, J., Jayabal, S., Chung, A. J., Watt, A. J., Sjöström, P. J. and van Meyel, D. J. (2014). Neuronal morphometry directly from bitmap images. *Nat. Methods* **11**, 982-984.

Fiala, J. C., Spacek, J. and Harris, K. M. (2002). Dendritic spine pathology: cause or consequence of neurological disorders? *Brain Res. Brain Res. Rev.* **39**, 29-54.

Fink, C. C., Bayer, K.-U., Myers, J. W., Ferrell, J. E., Jr, Schulman, H. and Meyer, T. (2003). Selective regulation of neurite extension and synapse formation by the beta but not the alpha isoform of CaMKII. *Neuron* **39**, 283-297.

Friedrich, P. and Aszódi, A. (1991). MAP2: a sensitive cross-linker and adjustable spacer in dendritic architecture. *FEBS Lett.* **295**, 5-9.

Ho, H.-Y. H., Susman, M. W., Bikoff, J. B., Ryu, Y. K., Jonas, A. M., Hu, L., Kuruvilla, R. and Greenberg, M. E. (2012). Wnt5a-Ror-Dishevelled signaling constitutes a core developmental pathway that controls tissue morphogenesis. *Proc. Natl. Acad. Sci. USA* **109**, 4044-4051.

Hsieh, J.-C., Rattner, A., Smallwood, P. M. and Nathans, J. (1999). Biochemical characterization of Wnt-frizzled interactions using a soluble, biologically active vertebrate Wnt protein. *Proc. Natl. Acad. Sci. USA* **96**, 3546-3551.

Hua, Z. L., Jeon, S., Caterina, M. J. and Nathans, J. (2014). Frizzled3 is required for the development of multiple axon tracts in the mouse central nervous system. *Proc. Natl. Acad. Sci. USA* **111**, E3005-E3014.

Ishida, A., Kameshita, I., Okuno, S., Kitani, T. and Fujisawa, H. (1995). A novel highly specific and potent inhibitor of calmodulin-dependent protein kinase II. *Biochem. Biophys. Res. Commun.* **212**, 806-812.

Ji, Y., Pang, P. T., Feng, L. and Lu, B. (2005). Cyclic AMP controls BDNF-induced TrkB phosphorylation and dendritic spine formation in mature hippocampal neurons. *Nat. Neurosci.* **8**, 164-172.

Kaufmann, W. E. and Moser, H. W. (2000). Dendritic anomalies in disorders associated with mental retardation. *Cereb. Cortex* **10**, 981-991.

Keeble, T. R. and Cooper, H. M. (2006). Ryk: a novel Wnt receptor regulating axon pathfinding. *Int. J. Biochem. Cell Biol.* **38**, 2011-2017.

Kellner, Y., Godecke, N., Dierkes, T., Thieme, N., Zagrebelsky, M. and Korte, M. (2014). The BDNF effects on dendritic spines of mature hippocampal neurons depend on neuronal activity. *Front. Synaptic Neurosci.* **6**, 5.

Kelly, P. T. and Vernon, P. (1985). Changes in the subcellular distribution of calmodulin-kinase II during brain development. *Brain Res.* **350**, 211-224.

Kim, J.-Y., Ash, R. T., Ceballos-Diaz, C., Levites, Y., Golde, T. E., Smirnakis, S. M. and Jankowsky, J. L. (2013). Viral transduction of the neonatal brain delivers controllable genetic mosaicism for visualising and manipulating neuronal circuits in vivo. *Eur. J. Neurosci.* **37**, 1203-1220.

Kulkarni, V. A. and Firestein, B. L. (2012). The dendritic tree and brain disorders. *Mol. Cell. Neurosci.* **50**, 10-20.

Lee-Hoeflich, S. T., Causing, C. G., Podkowa, M., Zhao, X., Wrana, J. L. and Attisano, L. (2004). Activation of LIMK1 by binding to the BMP receptor, BMPRII, regulates BMP-dependent dendritogenesis. *EMBO J.* **23**, 4792-4801.

Lyuksyutova, A. I., Lu, C. C., Milanesio, N., King, L. A., Guo, N., Wang, Y., Nathans, J., Tessier-Lavigne, M. and Zou, Y. (2003). Anterior-posterior guidance of commissural axons by Wnt-frizzled signaling. *Science* **302**, 1984-1988.

Marcos, S., Nieto-Lopez, F., Sandonis, A., Cardozo, M. J., Di Marco, F., Esteve, P. and Bovolenta, P. (2015). Secreted frizzled related proteins modulate pathfinding and fasciculation of mouse retina ganglion cell axons by direct and indirect mechanisms. *J. Neurosci.* **35**, 4729-4740.

Mardones, M. D., Andaur, G. A., Varas-Godoy, M., Henriquez, J. F., Salech, F., Behrens, M. I., Couve, A., Inestrosa, N. C. and Varela-Nallar, L. (2016). Frizzled-1 receptor regulates adult hippocampal neurogenesis. *Mol. Brain* **9**, 29.

McLeod, F., Bossio, A., Marzo, A., Ciani, L., Sibilla, S., Hannan, S., Wilson, G. A., Palomer, E., Smart, T. G., Gibb, A. et al. (2018). Wnt signaling mediates LTP-dependent spine plasticity and AMPAR localization through frizzled-7 receptors. *Cell Rep.* **23**, 1060-1071.

Meijering, E., Jacob, M., Sarria, J.-C. F., Steiner, P., Hirling, H. and Unser, M. (2004). Design and validation of a tool for neurite tracing and analysis in fluorescence microscopy images. *Cytometry A* **58A**, 167-176.

Morello, F., Prasad, A. A., Rehberg, K., Vieira de Sa, R., Anton-Bolanos, N., Leyva-Diaz, E., Adolfs, Y., Tissir, F., Lopez-Bendito, G. and Pasterkamp, R. J. (2015). Frizzled3 controls axonal polarity and intermediate target entry during striatal pathway development. *J. Neurosci.* **35**, 14205-14219.

Nakata, T. and Hirokawa, N. (1987). Cytoskeletal reorganization of human platelets after stimulation revealed by the quick-freeze deep-etch technique. *J. Cell Biol.* **105**, 1771-1780.

Povelones, M. and Nusse, R. (2005). The role of the cysteine-rich domain of Frizzled in Wingless-Armadillo signaling. *EMBO J.* **24**, 3493-3503.

Rodriguez, J., Esteve, P., Weinl, C., Ruiz, J. M., Fermin, Y., Trousse, F., Dwivedy, A., Holt, C. and Bovolenta, P. (2005). SFRP1 regulates the growth of retinal ganglion cell axons through the Fz2 receptor. *Nat. Neurosci.* **8**, 1301-1309.
Rosso, S. B. and Inestrosa, N. C. (2013). WNT signaling in neuronal maturation and synaptogenesis. *Front. Cell Neurosci.* **7**, 103.
Rosso, S., Bollati, F., Bisbal, M., Peretti, D., Sumi, T., Nakamura, T., Quiroga, S., Ferreira, A. and Cáceres, A. (2004). LIMK1 regulates Golgi dynamics, traffic of Golgi-derived vesicles, and process extension in primary cultured neurons. *Mol. Biol. Cell* **15**, 3433-3449.
Rosso, S. B., Sussman, D., Wynshaw-Boris, A. and Salinas, P. C. (2005). Wnt signaling through Dishevelled, Rac and JNK regulates dendritic development. *Nat. Neurosci.* **8**, 34-42.
Sahores, M., Gibb, A. and Salinas, P. C. (2010). Frizzled-5, a receptor for the synaptic organizer Wnt7a, regulates activity-mediated synaptogenesis. *Development* **137**, 2215-2225.
Salama-Cohen, P., Arevalo, M.-A., Grantyn, R. and Rodriguez-Tebar, A. (2006). Notch and NGF/p75NTR control dendrite morphology and the balance of excitatory/inhibitory synaptic input to hippocampal neurones through Neurogenin 3. *J. Neurochem.* **97**, 1269-1278.
Scheetz, A. J., Prusky, G. T. and Constantine-Paton, M. (1996). Chronic NMDA receptor antagonism during retinotopic map formation depresses CaM kinase II differentiation in rat superior colliculus. *Eur. J. Neurosci.* **8**, 1322-1328.
Shelly, M., Cancedda, L., Lim, B. K., Popescu, A. T., Cheng, P.-L., Gao, H. and Poo, M.-M. (2011). Semaphorin3A regulates neuronal polarization by suppressing axon formation and promoting dendrite growth. *Neuron* **71**, 433-446.
Shimogori, T., VanSant, J., Paik, E. and Grove, E. A. (2004). Members of the Wnt, Fz, and Frp gene families expressed in postnatal mouse cerebral cortex. *J. Comp. Neurol.* **473**, 496-510.
Umbhauer, M., Djiane, A., Goisset, C., Penzo-Mendez, A., Riou, J. F., Boucaut, J. C. and Shi, D. L. (2000). The C-terminal cytoplasmic Lys-thr-X-X-X-Trp motif in frizzled receptors mediates Wnt/beta-catenin signalling. *EMBO J.* **19**, 4944-4954.
Vaillant, A. R., Zanassi, P., Walsh, G. S., Aumont, A., Alonso, A. and Miller, F. D. (2002). Signaling mechanisms underlying reversible, activity-dependent dendrite formation. *Neuron* **34**, 985-998.
Valnegri, P., Puram, S. V. and Bonni, A. (2015). Regulation of dendrite morphogenesis by extrinsic cues. *Trends Neurosci.* **38**, 439-447.
Van Aelst, L. and Cline, H. T. (2004). Rho GTPases and activity-dependent dendrite development. *Curr. Opin. Neurobiol.* **14**, 297-304.
Varela-Nallar, L., Grabowski, C. P., Alfaro, I. E., Alvarez, A. R. and Inestrosa, N. C. (2009). Role of the Wnt receptor Frizzled-1 in presynaptic differentiation and function. *Neural Dev.* **4**, 41.
Varela-Nallar, L., Ramirez, V. T., Gonzalez-Billault, C. and Inestrosa, N. C. (2012). Frizzled receptors in neurons: from growth cones to the synapse. *Cytoskeleton* **69**, 528-534.
Wang, Y., Huso, D., Cahill, H., Ryugo, D. and Nathans, J. (2001). Progressive cerebellar, auditory, and esophageal dysfunction caused by targeted disruption of the frizzled-4 gene. *J. Neurosci.* **21**, 4761-4771.
Wayman, G. A., Lee, Y.-S., Tokumitsu, H., Silva, A. J. and Soderling, T. R. (2008). Calmodulin-kinases: modulators of neuronal development and plasticity. *Neuron* **59**, 914-931.
Wen, Z., Guirland, C., Ming, G.-L. and Zheng, J. Q. (2004). A CaMKII/calcineurin switch controls the direction of Ca(2+)-dependent growth cone guidance. *Neuron* **43**, 835-846.
Withers, G. S., Higgins, D., Charette, M. and Banker, G. (2000). Bone morphogenetic protein-7 enhances dendritic growth and receptivity to innervation in cultured hippocampal neurons. *Eur. J. Neurosci.* **12**, 106-116.
Witte, H. and Bradke, F. (2008). The role of the cytoskeleton during neuronal polarization. *Curr. Opin. Neurobiol.* **18**, 479-487.
Wong, H.-C., Bourdelas, A., Krauss, A., Lee, H.-J., Shao, Y., Wu, D., Mlodzik, M., Shi, D.-L. and Zheng, J. (2003). Direct binding of the PDZ domain of Dishevelled to a conserved internal sequence in the C-terminal region of Frizzled. *Mol. Cell* **12**, 1251-1260.
Wu, G.-Y. and Cline, H. T. (1998). Stabilization of dendritic arbor structure in vivo by CaMKII. *Science* **279**, 222-226.
Yu, X. and Malenka, R. C. (2003). Beta-catenin is critical for dendritic morphogenesis. *Nat. Neurosci.* **6**, 1169-1177.
Yu, H., Ye, X., Guo, N. and Nathans, J. (2012). Frizzled 2 and frizzled 7 function redundantly in convergent extension and closure of the ventricular septum and palate: evidence for a network of interacting genes. *Development* **139**, 4383-4394.
Zoghbi, H. Y. (2003). Postnatal neurodevelopmental disorders: meeting at the synapse? *Science* **302**, 826-830.

Fig. S1. Fz7 rescues the defects on dendritic complexity induced by Fz7 blockage. (A) Representative images of 3 DIV neurons expressing EGFP, Fz7 shRNA or both Fz7 shRNA and MycFz7. Quantification shows total dendritic length (B) and TDBTN (C) for each condition. **** $p<0.0001$ compared to EGFP and ++++ $p<0.0001$ compared to Fz7 shRNA. (D and E) Quantitative analysis of total dendritic length and TDBTN from EGFP or ssRNA expressing neurons. Error bars represent mean ± SEM. Scale bar: 10 μm.